Sputter Theory

Herbert M. Urbassek*

Fachbereich Physik, Universität Kaiserslautern
Erwin-Schrödinger-Straße, D-67663 Kaiserslautern, Germany

Abstract

Progress in the description of energetic-particle-induced sputter processes is predominantly based on computer simulation techniques. This review reports on the progress reached in long standing issues, such as the nature of sputtering from spikes. and highlights research areas which are now actively being investigated, such as topography changes in the irradiated surface induced by sputtering and its consequences upon sputtering.

Contents

* E-mail: urbassek@rhrk.uni-kl.de

1. Introduction: Available Theoretical Tools

The theoretical understanding of sputter processes has a long history, cf. the introductory chapter of Sigmund (1981). Since the introduction of transport-theoretic methods into this field in the 1960s, and culminating in the seminal paper by Sigmund (1969), a great variety of problems have been analyzed using this method, such as the dependence of the total sputter yield on ion impact energy, angle and species as well as the target materials parameters; the energy and angular distributions of sputtered particles; the preferential sputtering of alloys and compounds; and the depth of origin of emitted particles. Progress in the field of sputtering has been summarized in Behrisch (1981, 1983), Behrisch and Wittmaack (1991) and Sigmund (1993). A recent review over the field is given in the Proceedings of the Grove Symposium (2004), and here in particular in the survey by Baragiola (2004).

These analytical studies allowed to obtain a systematic and explicit quantitative understanding, which in many cases adequately covered the phenomena described above. They were soon supplemented and extended by computer simulation methods (Eckstein, 1991). Here binary-collision codes were among the first to be developed. These are similar in spirit to the analytical transport theory in that they ignore multiple atom interaction, but concentrate on the close collisions dominating projectile slowing down and recoil generation. Prominent examples of these codes are TRIM (Biersack and Haggmark, 1980; Biersack and Eckstein, 1984), in which the target crystal structure is ignored and thus an amorphous target is modelled, and MARLOWE (Robinson and Torrens, 1974), which takes full account of target crystallinity. These codes were developed in the 1970s and 1980s and

applied to the issues of sputter theory mentioned above. The results obtained were generally in good agreement with analytical theory. Additionally, in specific areas, which are difficult to treat using transport theory, these codes brought new insight, such as for low projectile energies, including the regime of single-knockon (near-threshold) sputtering, and in particular when covering the effects of target crystallinity. Also the issue of the fluence dependence of sputtering, which is of particular importance for compound targets, which undergo stoichiometry changes under sputtering, could be naturally included in such codes; here TRIDYN is a prominent example (Möller and Eckstein, 1984). Nowadays, an essential role played by these codes is their widespread availability for experimentalists, which allows them to quickly estimate projectile ranges, sputter yields, etc.

Another theoretical tool consists of the method of molecular-dynamics simulation, in which the interaction of each (projectile or target) atom with all surrounding atoms is taken into account. This method is expected to give the most realistic description of particle slowing down, recoil generation, and sputtering. Molecular dynamics has been employed already in the 1970s, in particular by the pioneering work of Harrison and coworkers (Harrison, 1988). The initial restriction of this method to small target sizes and thus small impact energies – which was dictated by CPU time and memory restrictions – was gradually relieved by the progress in available computer hardware. Thus this method has experienced a considerable progress in the 1990s (Urbassek, 1997), which continues until today. It allowed to attack questions in which multiple atom interaction is important. This applies in particular to the so-called spike regions, which are defined as "a limited volume with the majority of atoms temporarily in motion" (Sigmund, 1974). Since this tool does not only describe repulsive events ("collisions") but also the environment- and configuration-dependent attraction between particles, it has been used to study a variety of sputter phenomena such as the influence of surface topography on sputtering, creation of surface defects by sputtering, cluster emission, or chemical effects in sputtering.

In this review, I will highlight the areas upon which research in sputter theory now focuses. Since most issues of collision-cascade sputtering have been treated satisfactorily, research now generally aims at a detailed quantitative agreement between experiment and theory in specific systems, while most basic questions appear to have been adequately settled. This review will cover the field of projectile impact in the nuclear-stopping regime, while processes of so-called electronic or chemical sputtering are only briefly addressed in Sections 3.5 and 4.3, respectively. Furthermore, with the exception of Section 2.7, which treats

irradiation-induced composition changes, I will concentrate on "static" results, i.e., omit aspects of the fluence dependence of sputtering.

2. Collision Cascades

The concept of a linear collision cascade describes how the projectile energy is distributed among target atoms via a series of collision events; in each of these, an energetic atom collides with an atom at rest and conveys part of its energy to it. We note that early after projectile impact the collision cascade will usually be linear since the density of moving recoil atoms is low. With increasing time, however, this density increases and the cascade becomes nonlinear. Often, however, this latter phase has no influence on sputtering, if the recoil energies are too small (i.e., smaller than the surface binding energy).

2.1. Yield

Linear cascade theory predicts the sputter yield Y to obey

$$Y = \frac{1}{8} \frac{\Gamma_m F_D \Delta x}{U}, \tag{1}$$

where Γ_m is a number, which slightly depends on the low-energy interaction potential, U is the surface binding energy, Δx is the depth of origin of sputtered atoms, and F_D is the energy deposited near the surface. F_D is proportional to the nuclear stopping power of the projectile.

Figure 1 presents a compilation of experimental data of the sputter yields of Si, which shows good quantitative agreement with the ideas underlying Equation (1). This was possible by (i) introducing a reduced energy ϵ, which scales the bombarding energy by parameters depending on the projectile and target atom species, and a reduced stopping power $s_n(\epsilon)$; (ii) writing Equation (1) as $Y = C \cdot s_n(\epsilon)$, where C contains all remaining (energy-independent) factors of Equation (1), (iii) taking threshold effects into account, cf. Section 2.4 below.

So, in general, Equation (1) well describes the physics underlying sputtering in the collision cascade regime.

2.2. Energy Distributions

Collision cascade theory predicts the energy spectrum of sputtered particles to be given by a law

$$f(E) \propto \frac{E}{(E+U)^{3-2m}}, \tag{2}$$

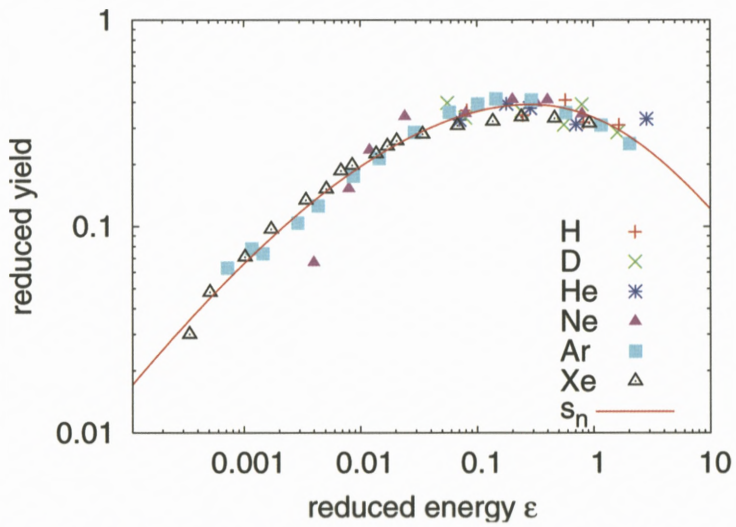

Figure 1. Compilation of experimentally determined sputter yields of Si with normally incident ions. The reduced sputter yields, $y = Y/C$, cf. Section 2.1, have been plotted *versus* the reduced energy ϵ and are seen to align well with the reduced nuclear stopping cross section s_n. Threshold effects have been taken into account via the factor η, Equation (4). Compilation and analysis due to Wittmaack (2003).

where m is a parameter characterizing the repulsive part of the interatomic interaction potential valid in the range of energies of sputtered particles. m is in the range of 0–0.2. Figure 2 gives an example showing that sputtered particle spectra can be well fitted using this law. We note, however, that in such fits, usually both U and m are used as fit parameters. Deviations of the fit value of U to the cohesive energy or sublimation energy of the solid are often ascribed to surface roughness or impurities. From a theoretical point of view, the surface binding energy of single-crystalline flat surfaces is readily calculated; its relevance for describing the energy loss of sputtered particles has been discussed by Gades and Urbassek (1992) for elemental metals and in (1994b) for alloys.

2.3. Angular Distribution

Analytical theory predicts the collision cascade to become isotropic, resulting in a cosine distributed flux of the sputtered atoms. At small projectile energies, below 1 keV, say, the collision cascade still remembers the initial momentum of the projectile; for perpendicular incidence the flux of sputtered atoms is undercosine, i.e., particles are preferentially sputtered at oblique angles rather than perpendicular to the surface. This prediction is in general found to be true.

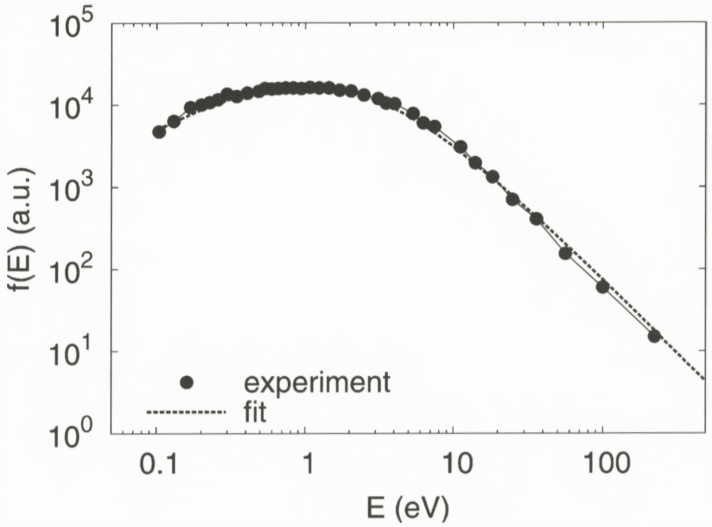

Figure 2. Kinetic energy distribution of neutral Ag atoms sputtered from a polycrystalline Ag sample by bombardment with 5 keV Ar ions at 45° impact angle. Fit to Equation (2) with surface binding energy $U = 2.94$ eV and power exponent $m = 0.15$. Data taken from Wahl and Wucher (1994).

In theoretical terms, this issue has been discussed with the help of the so-called *deposited-momentum* distribution in the collision cascade (Sckerl et al., 1996). In analogy to the well known deposited-energy distribution, it quantifies the space dependence of the average momentum (vector) of recoil atoms, and hence the anisotropy of the collision cascade.

Deviations from the cosine distribution may also be caused by other reasons:

1. Crystal effects play a dominant role in the establishment of the angular distribution (Hofer, 1991; Rosencrance et al., 1995).
2. Impurities present at the surface and also projectiles implanted there disturb the angular distribution.
3. When experiments are performed under high fluences, often a tendency to an over-cosine distribution is found, i.e., a higher emission probability in the normal direction; this feature is usually connected to the evolution of surface topography under higher fluence bombardment.

In particular the first effect mentioned above, viz. the influence of the crystalline structure, is rather complex, as for instance the detailed and systematic experimental investigation of the sputtering of the Au (111) surface in its depen-

dence on ion species, ion energy, and temperature by Szymczak and Wittmaack (1993) demonstrates. The available published modelling, such as the work by Hou and Eckstein (1990), extends only over a small fraction of the parameter space investigated experimentally.

2.4. Low-Energy Bombardment

Small impact energies E_0 lead to characteristic deviations from fully established collision cascades:

1. The energy spectrum is steeper than $1/E^2$.
2. The angular distribution is non-isotropic, favouring emission angles in the direction of the projectile.
3. The sputter yield exhibits a threshold at an energy E_{th}.

In particular the sputter threshold energy E_{th} and the energy dependence of the sputter yield in its vicinity have been the subject of several investigations. Here in general empirical laws have been formulated by various authors. One of these, which has been implemented in Figure 1, is due to Bohdansky (1984) and reads

$$Y_{\text{th}}(E_0) = \left(\frac{1}{8}\,\frac{\Gamma_m F_D \Delta x}{U}\right) \cdot \eta\left(\frac{E_{\text{th}}}{E_0}\right), \tag{3}$$

where the first term in brackets on the right is the sputter yield of Equation (1) and $\eta(x)$ denotes the threshold function

$$\eta(x) = (1 - x^{2/3})(1 - x)^2, \quad (0 < x < 1). \tag{4}$$

The threshold energy, at which sputtering sets in rather sharply, has been derived by Eckstein et al. (1993) to depend on the surface binding energy U and on the mass ratio $\mu = M_2/M_1$ of the target atom mass M_2 to the projectile ion mass M_1 as

$$\frac{E_{\text{th}}}{U} = 7.0\mu^{-0.54} + 0.15\mu^{1.12}. \tag{5}$$

As Figure 1 shows, the inclusion of the threshold function leads to a satisfactory agreement between experiment and theory.

2.5. Depth of Origin

The depth of origin, Δx, has been introduced in Equation (1) as a length characterizing the depth out of which recoils may be ejected. With the exponent m describing the interaction potential of low-energy recoils, it reads

$$\Delta x = \frac{1}{1-2m}\frac{1}{NC_m}U^{2m} \tag{6}$$

and is hence proportional to the range of a recoil of energy U. Since for low-energy recoils, $m = 0$, Equation (6) gives the average depth of origin as

$$\Delta x = \frac{1}{NC_0}. \tag{7}$$

With the original value of the low-energy stopping cross section C_0, this resulted in 5 Å (Sigmund, 1969). However, this value has been recalculated by Vicanek et al. (1989) who found that C_0 should be increased by a factor of 2, thus resulting in a depth of origin of $\Delta x = 2.5$ Å. Glazov et al. (1998) and Shulga and Eckstein (1998) demonstrated by computer simulations that the escape depth is a factor of 4 smaller than the original estimate by Sigmund (1969). This is in reasonable agreement with experimental data by Wittmaack (1997, 2003), who showed particles to be mainly sputtered from the topmost surface layer. We note that the computer simulations of Shulga and Eckstein (1998) predict a dependence on the atomic number density proportional to $N^{-0.86}$ instead of N^{-1} as in Equations (6) and (7).

2.6. Preferential Sputtering

The sputtering behaviour of compounds and alloys is of considerable practical interest. Let us concentrate on the sputtering of a binary system of species i and j which are homogeneously mixed with concentrations c_i, c_j, where $c_i + c_j = 1$. The normalized ratio

$$\delta = \frac{Y_i}{Y_j}\frac{c_j}{c_i} \tag{8}$$

is called the sputter preferentiality, since its deviation from the value 1 indicates over- or under-stoichiometric emission of a particular species. Analytical sputter theory (Sigmund, 1981) predicts δ to depend on the masses $M_{i,j}$ and the surface binding energies $U_{i,j}$ of the respective species in the alloy as

$$\delta = \left(\frac{M_j}{M_i}\right)^{2m}\left(\frac{U_j}{U_i}\right)^{1-2m}. \tag{9}$$

Here m denotes the power exponent describing the interaction potential.

A special case of particular interest is the sputtering of isotopic mixtures. Here sputtering is governed by the mass ratios of the different isotopes in the specimen. Equation (9) thus predicts a preferentiality

$$\delta = \left(\frac{M_j}{M_i}\right)^{2m} . \tag{10}$$

Since this effect is small, in simulations the mass difference is often artificially enhanced. Early work by Shapiro et al. (1988) and Lo et al. (1989) and more recent simulations by Gades and Urbassek (1995) obtained preferentialities compatible with the experimental findings and Equation (10).

Shulga and Sigmund (1995, 1996) performed a series of simulations, where besides binary-collision simulations also molecular dynamics was employed. Molybdenum isotope samples with an artificially increased mass ratio were investigated. These authors studied in particular the dependence of the preferentiality on the bombarding ion energy, and showed that the theoretical result is only retrieved for high energies ($E_0 > 10$ keV in their case). At low bombarding energies, the sputter preferentiality strongly depends on the mass and energy of the bombarding species and varies considerably with the emission angle; this effect could be reduced to the collision kinematics of binary scattering.

2.7. Irradiation-Induced Composition Changes

After long-term bombardment, the surface composition of the target changes. This has several causes: Besides the preferential sputtering effect itself, collisional mixing in the target, radiation-enhanced diffusion and Gibbsian and radiation-induced segregation change the target composition. Furthermore, the altered concentrations and atomic densities in the target may lead to strong local pressures; thus the effect of the relaxation of this pressure needs to be taken into account. The review by Sigmund and Lam (1993) summarizes the underlying physics and presents a comprehensive theoretical framework for analyzing these processes quantitatively. As a consequence of the altered composition profile, also the sputter yields and their preferentiality will be changed as a function of fluence.

Conrad and Urbassek (1992) give a detailed analysis of this effect by taking collisional mixing, preferential sputtering and pressure relaxation in the target self-consistently into account. They investigate a $^{70}Ge/^{76}Ge$ mixture irradiated by 5 keV Ar ions in the framework of a Monte Carlo study. A steady-state concentration profile develops after one ion range has been sputtered away; then the light isotope is depleted at the surface and the sputter preferentiality becomes unity, as

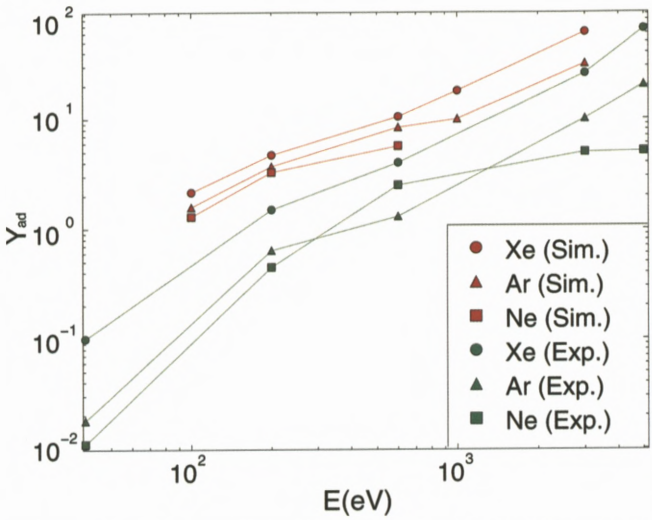

Figure 3. Comparison of simulation data (Gades and Urbassek, 1994a) and experimental data (Michely and Teichert, 1994) of adatoms produced by energetic rare-gas ion bombardment of a Pt (111) surface.

it must be in steady state. These results are in close qualitative agreement with experiments by Gnaser and Oechsner (1990).

In a more comprehensive study, in which all the effects mentioned above are included, Sckerl et al. (1998) investigate in detail the compositional changes in alloys, such as NiCu, and compare to experimental data. Since these authors also allow for higher target temperatures, up to 700°C, the effects of Gibbsian segregation and radiation-enhanced diffusion on the concentration profiles become considerable and even dominant. In a related paper, Vicanek et al. (1998) investigate the effect of composition gradients in alloys on preferential sputtering. This theoretical analysis finds that a surface-depleted species is emitted preferentially in normal direction; they identify a *neutral angle*, where the composition of the sputter flux is representative of the entire flux emitted in the half space.

2.8. Creation of Surface Topography

This topic has gained increasing attention due to the necessity of modelling the evolution of surface topography with ion fluence. Figure 3 gives an example of the formation of adatoms due to keV ion bombardment of a metal surface. An atomistic understanding of the effect of an individual ion-induced collision cascade on the surface topography appears useful, as shown by the contributions

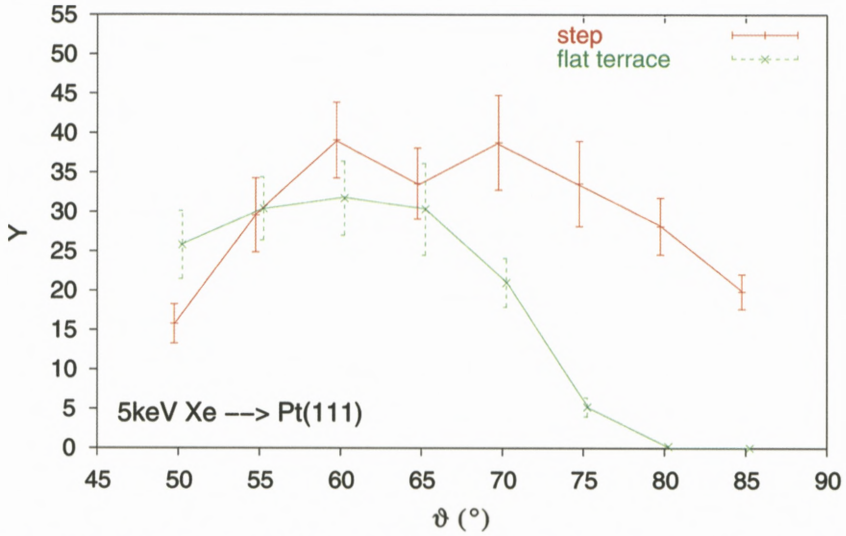

Figure 4. 5 keV Xe impact on a Pt (111) surface: Dependence of the sputter yield Y on the incidence angle ϑ. Data for ion impact on a flat terrace, and on a stepped surface with impact point into the unit cell immediately in front of the step edge. Lines are to guide the eye. Data taken from a molecular-dynamics simulation by Friedrich (2003); for details see also Friedrich and Urbassek (2003).

of Chason and Chan (2006) and Aziz (2006) in these proceedings. One possible approach consists in calculating the *average* surface height profile around the ion impact point using a binary-collision or a molecular-dynamics simulation. Here more work is necessary to obtain this distribution in analytical form and parametrized with the relevant projectile and target materials parameters. Such an analytical representation is necessary for implementation into the (stochastic) equations governing surface evolution.

2.9. Influence of Surface Topography on Sputtering

Both the analytical theory of sputtering and most simulation codes aim at describing sputtering from a planar target surface. However, it has become more and more interesting to describe the effect of target surface structure on sputtering:

1. On a microscopic level, target surfaces are not planar, except in rare cases, where the surface to bombard has been characterized carefully before bombardment. Usually, the surface is atomically rough and full of defects. Conversely, with the advent of scanning tunnelling microscopy techniques, it has become possible to characterize sputtering events individually on an

atomic scale. Figure 4 gives an example of how the presence of a surface step influences the sputter yield, in particular for glancing-ion incidence.

2. After prolonged sputtering, even an initially flat surface will develop roughness. Furthermore, in a number of interesting cases, a surface instability results, which leads to ripple or nanodot formation on the surface.
3. With the advent of nanotechnology, it has become relevant to characterize the sputtering behaviour of nanoscopic structures on surfaces – e.g., trenches, grooves, ridges, edges, etc.

Already quite early, Sigmund (1973) characterized the curvature dependence of the sputter yield. This description is today the basic ingredient of the theories describing surface-structure formation under sputtering (Bradley and Harper, 1988; Michely and Krug, 2004; Chason and Chan, 2006). Figure 5 gives an atomistic example, in which the sputtering of a flat Au surface by 16 keV Au ions is compared to that of a spherical Au cluster with diameter 20 nm. Both the sputter yield and the time evolution of sputtering in the two cases are quite different. The range of the projectile is in this case around of third of the curvature radius of the cluster.

2.10. Progress in Transport Theory

As mentioned in the Introduction, transport theory formed the starting point for sputter theory (for a recent review, see Jakas, 2004). This approach has the obvious advantage of delivering systematic results, in which the important sputter parameters are included in a transparent analytical way, such as for instance in Equation (1). The complexity of the underlying integro-differential equation necessitated several simplifications, notably in the cross sections employed (the so-called *power-law* cross sections are used as a rule) and in the assumption of an *infinite target*, in which the surface only forms a reference plane rather than a boundary. Furthermore, the results obtained apply to the *asymptotic* regime, where the recoil energy E is small compared to the bombarding energy E_0; here, in particular, the cascade becomes isotropic.

It turned out that the dismissal of any of these assumptions requires considerable effort and sometimes the introduction of novel theoretical concepts. However, important progress could be reached in the following areas:

1. Glazov (1994a, 1994b, 1995) reanalyzed the problem of the space dependence of the deposited energy distribution, which is basic to the description of the sputter yield, Equation (1), and of the related concept of the deposited momentum distribution. In particular, he succeeded (1997) to calculate the

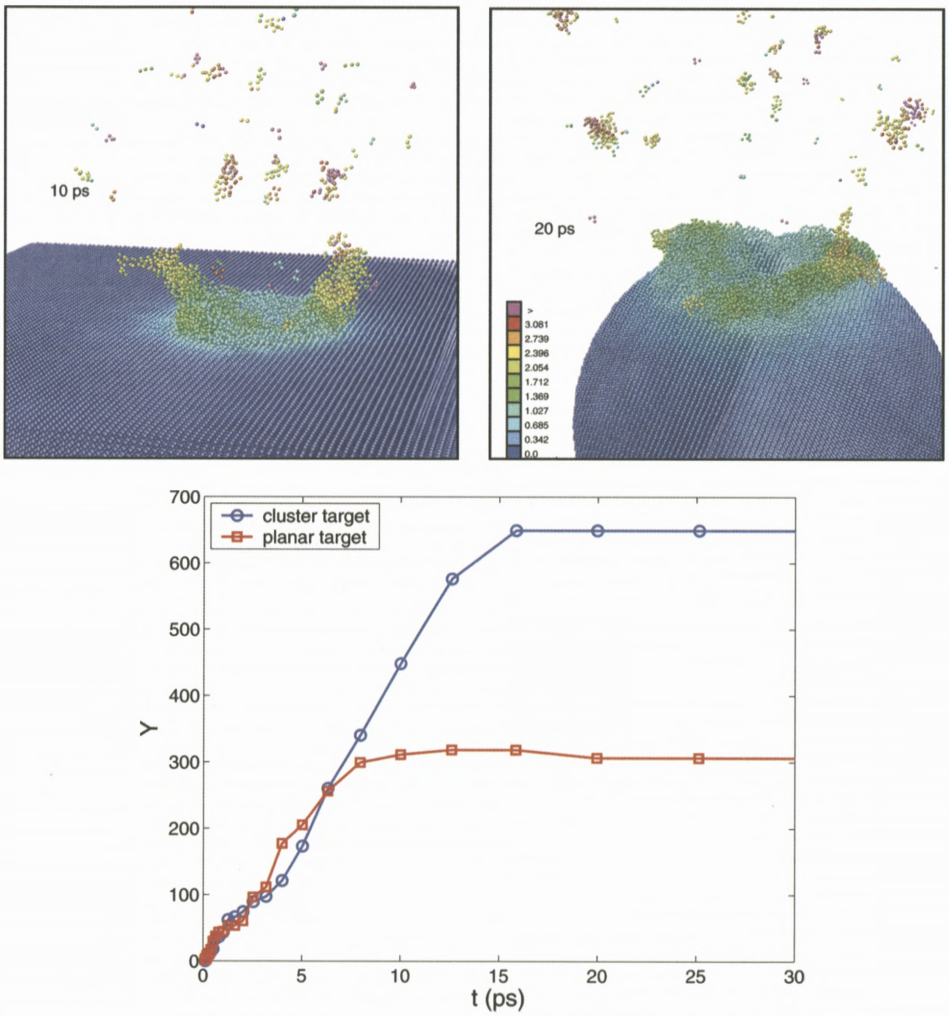

Figure 5. Comparison of the perpendicular impact of a 16 keV Au atom on (a) a planar Au surface, (b) a spherical Au cluster target with diameter 20 nm. The cluster has been bombarded centrally into a region which has a local (111) surface face. Representative sputter events with average sputter yields of 306 and 649, resp., have been selected. Colour denotes local temperature in 1000 K. (c) Comparison of the time evolution of the sputter yields. Courtesy of St. Zimmermann (2006).

sputter flux from a half-space medium. Here, he used the technique of *invariant embedding*, which is well known in other areas of transport theory, and subsequently turned out to be fruitful in several other problems of particle-solid interaction, such as electron (Vicanek, 1999) and positron (Glazov and Paszit, 2004) backscattering from surfaces.

2. The anisotropy of collision cascades – with the exclusion of crystal structure effects – has been analyzed systematically by Sckerl et al. (1996). Its two leading sources were identified as the projectile momentum and the gradient of the deposited energy density. Its relation with the so-called deposited momentum distribution was clarified.
3. Results on the sputtering of binary media, including in particular isotopic systems, have already been discussed in Section 2.6.
4. Asymptotically correct expressions for particle fluxes in binary media could be derived for general, i.e., non-power-law, cross sections by Vicanek et al. (1993).

3. Spikes

A general condition when spikes may contribute to sputtering is given by the criterion

$$E_{\text{atom}} \gtrsim U, \tag{11}$$

where E_{atom} is the energy per atom in the spike volume and U is the cohesive energy of the material. Such a condition may be reached for

1. heavy ion impacts on heavy targets, such as Au on Au,
2. in particular for cluster impact,
3. for weakly bonded solids such as condensed gas targets, weakly bonded molecular targets, etc.,
4. in swift-ion tracks.

3.1. Models

A number of models have been derived already in the 1980s (see Reimann, 1993, for a review) to explain sputtering by spikes with the help of continuum-mechanical, thermo- or hydro-dynamical models:

1. surface evaporation (Johnson and Evatt, 1980; Sigmund and Claussen, 1981),

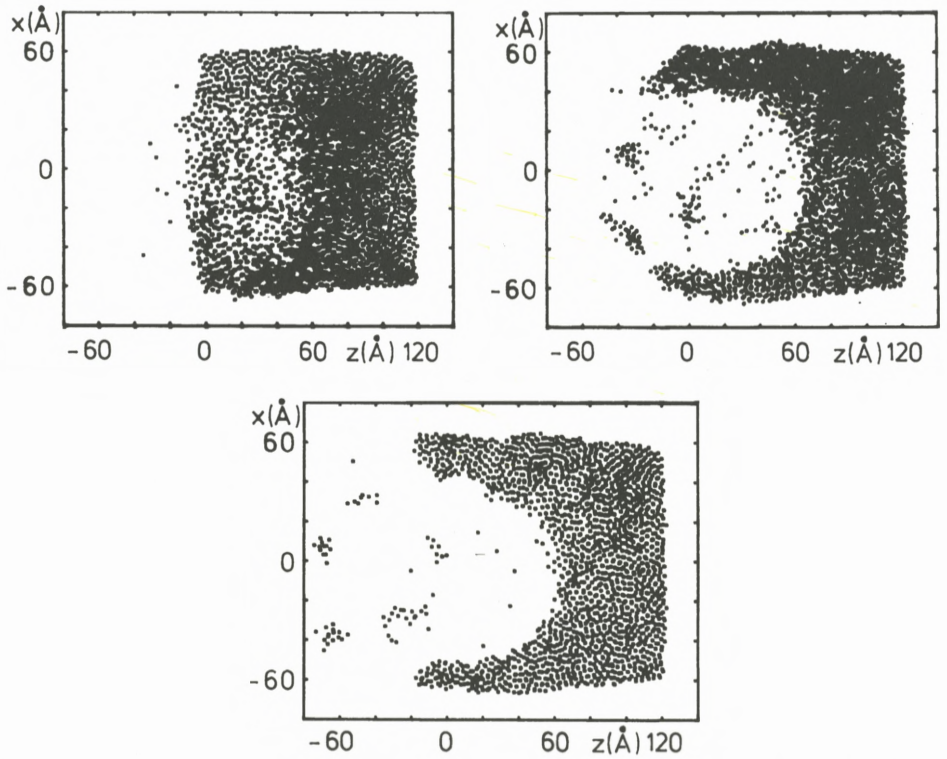

Figure 6. Time evolution of the density in an amorphous Ar solid irradiated at time $t = 0$ by a 1 keV Ar atom. Every dot represents an Ar atom in a layer extending 3.5 Å on both sides of the plane $y = 0$. The surface is initially at $z = 0$. (a) $t = 3.2$ ps after ion impact. (b) $t = 13.8$ ps. (c) $t = 24.7$ ps. Taken from Urbassek and Waldeer (1991).

2. phase explosion, also called bulk evaporation or gas flow (Urbassek and Michl, 1987; Sunner et al., 1988; Kelly, 1990),
3. shock wave (pressure pulse) (Kitazoe et al., 1981; Bitensky and Parilis, 1987; Johnson et al., 1989).

All these models emphasize one aspect which may be relevant for producing sputtering from a spike, while in reality several of the mechanisms proposed above may be operative simultaneously. In this area, molecular-dynamics simulations proved particularly useful in understanding the sputtering mechanisms, since in the simulations the effect of the high energy deposition is taken to account in an atomistic manner.

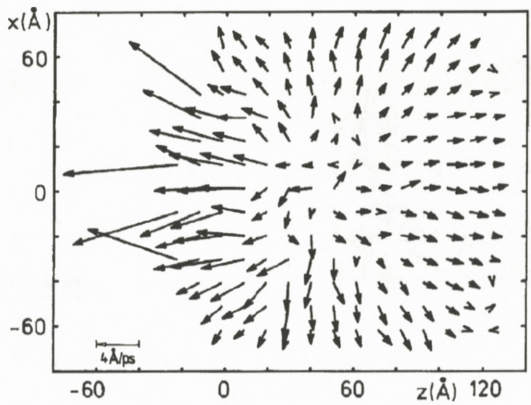

Figure 7. Velocity distribution corresponding to the earliest plot in Figure 6. Velocities are calculated as averages over a cubic cell of dimension $8 \times 7 \times 8$ Å^3. Only the projection of the velocities onto the plane $y = 0$ is plotted. Taken from Urbassek and Waldeer (1991).

In an early simulation of the sputtering of a condensed Ar target by 1 keV Ar atoms, Urbassek and Waldeer (1991) demonstrated the mechanisms of sputtering in a spike regime for the first time. Figure 6 shows that the entire collision-cascade region is filled with a high energy density, such that the kinetic energy surpasses the cohesive energy of an atom; in other words, the volume is heated above the critical point of the liquid-vapour phase transition. The high thermal pressure built up in the target then accelerates the atoms out of the cascade volume. Figure 7 displays the velocity distribution of the sputtered atoms and demonstrates the collective nature of flow. Thus this simulation gives evidence that sputtering occurs via the phase explosion mechanism mentioned as item 2 above. The shock wave plays no role in this case, since it runs *into* the material, thus causing no sputtering from the surface.

Figure 8a displays the energy distribution of sputtered particles for this event. Characteristically, besides a collision cascade contribution – applicable for emission energies above 0.1 eV – a strong low-energy contribution with a broad maximum for energies below around 20 meV is visible. This strong enhancement of low-energy sputtered particle has been found experimentally in many cases of spike sputtering, both for condensed-gas targets (Haring et al., 1984) and also for metals (Figure 8b).

Interestingly, the sputtering of metals under spike conditions follows the same pathway. This is demonstrated in Figure 9, where the sputtering of Au by 16 keV Au_4 cluster impact is shown. Again, the phase explosion mechanism is seen to be operative. Now, however, the liquid phase plays a more important role than in Ar:

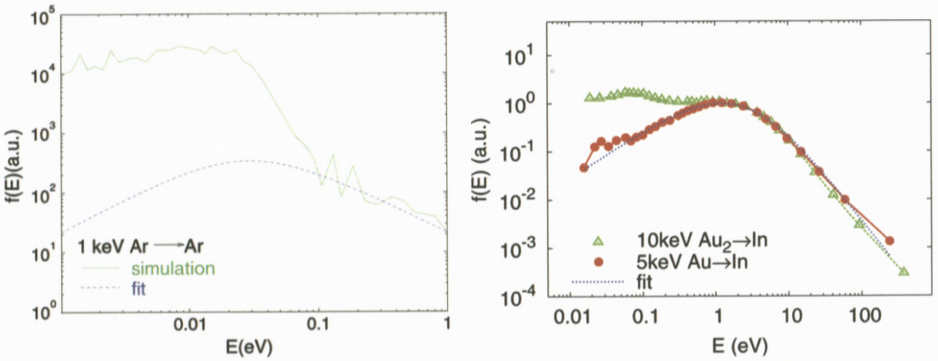

Figure 8. Energy distributions of particles sputtered from a spike, compared to the fit to a Thompson distribution of linear-cascade theory, Equation (2). (a) Molecular-dynamics data for 1 keV Ar → Ar bombardment Urbassek and Waldeer (1991). These data pertain to the individual impact event described in Figures 6 and 7, with a (particularly abundant) sputter yield of 911 atoms. (b) Experimental data Samartsev et al. (2005) of neutral In atoms sputtered from a polycrystalline In sample under impact of a Au atom (green triangles) and a Au_2 dimer (red circles). The impact energy is in both cases 5 keV/atom. The fit describes well the case of atom bombardment, but not the excess of low-energy atoms which are sputtered by dimer impact.

1. The walls of the forming crater are temporarily covered by a liquid film.
2. This liquid is driven out of the crater volume by the expansion; the temporarily forming protrusions or "fingers" (Nordlund et al., 2003) – irregular columns of liquid material protruding above the surface – have little heat contact to the target and therefore stay liquid and mobile for a long time (up to 100 ps). Eventually they may break away from the surface, forming large liquid droplets in the flux of emitted material, or fall back onto the surface forming large adatom islands. Both these phenomena are seen in experiment (Donnelly, 2006).

Effects of shock waves on sputtering do not appear to have been seen in simulations up to now. They may become important when the impact-induced spike is buried under the surface and emits a shock wave to the surface, which leads to the emission of solid chunks of material by a spallation mechanism; or in the bombardment of thin foils, where the shock wave may lead to (spallation) emission from the backside of the material. Such phenomena appear to have been seen by Rehn et al. (2001), cf. also Donnelly (2006). Interestingly the cluster size distribution observed in this group obeys a power law $Y(n) \propto n^{-\alpha}$ with $\alpha = 2$, corresponding to the value predicted by shock wave models (Bitensky and Parilis, 1987), cf. the discussion in Section 3.4.

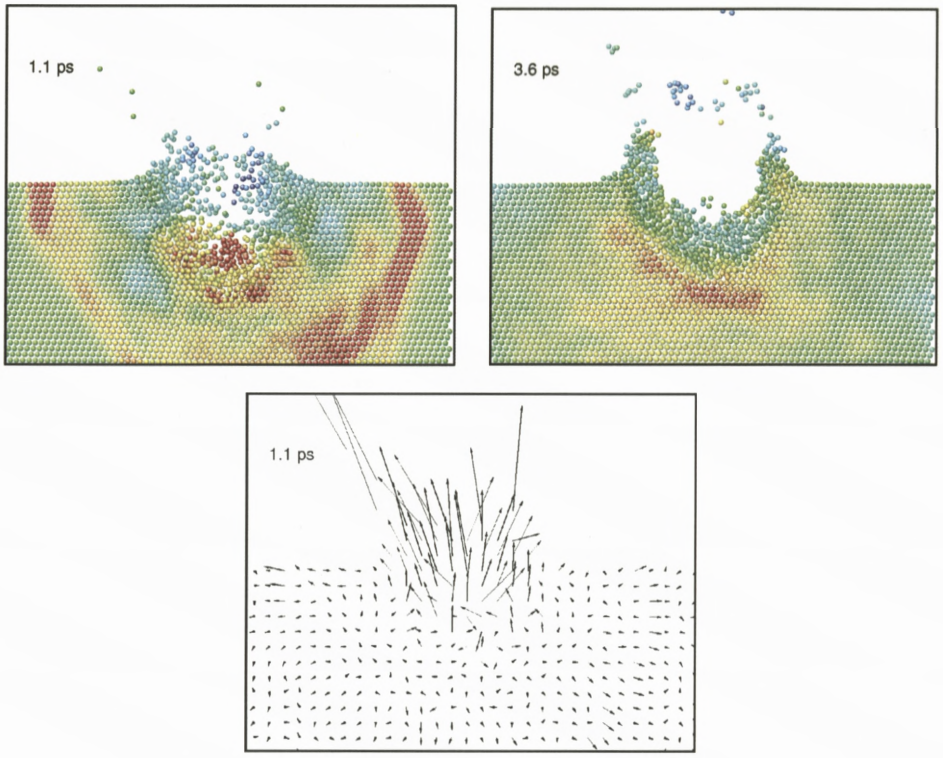

Figure 9. Molecular-dynamics data of a 16 keV Au_4 on Au. A representative event with a sputter yield of $Y = 317$ is shown. The data visualize the pressure distribution inside the target at 1.1 ps (a) and 3.6 ps (b) after impact. Yellow and red denotes compressive pressure, turquoise and blue tensile pressures. (c) Velocity profile of this event at 1.1 ps. Taken from Colla et al. (2000).

3.2. Cluster Impact

Similar considerations hold for the sputter yield due to cluster impact. If the impact velocity is relatively small, such that the energy deposition occurs close to the target surface, the sputter yield is more or less linear in the *total impact energy* of the cluster. This is exemplified in Figure 10 both for a condensed-Ar target and a metal. The sputter yield $Y_n(E)$ of a cluster projectile of size n with total energy E obeys in good approximation the law (Anders et al., 2004)

$$Y_n(E) = a\frac{\epsilon^{1+b}}{(\epsilon_{\mathrm{th}} + \epsilon)^b}, \tag{12}$$

where $\epsilon = E/U$. a, b and ϵ_{th} are constants denoting a "sputter efficiency", the onset of sputtering in the threshold regime, and the threshold energy, respectively.

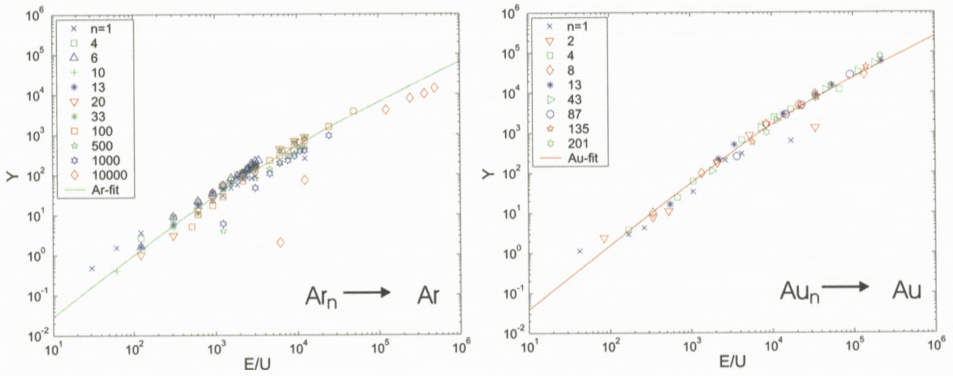

Figure 10. Synoptic display of self-sputter yield of cluster impact of (a) an Ar solid (Anders et al., 2004) and (b) a Au solid (Zimmermann and Urbassek, 2006). The bombarding energy E has been scaled to the cohesive energy of the target U. A fit function, Equation (12), with parameters as given in the text has been included.

Note that the cluster size n does not appear explicitly in Equation (12); it is only the total cluster energy that determines the yield. For high energies, Equation (12) simplifies to a linear law,

$$Y_n(E) = a(\epsilon - b\epsilon_{\text{th}}), \quad \epsilon \gg \epsilon_{\text{th}}. \tag{13}$$

Zimmermann and Urbassek (2006) find that the constants assume similar values for the two systems studied: $a = 0.065$ (0.246), $b = 0.54$ (0.60), and $\epsilon_{\text{th}} = 3160$ (10600) for an Ar (Au) target. The deviations between the two parameter sets may be due to the role of the liquid phase, which is more relevant for metals than for van-der-Waals bonded systems.

However, this simple finding disagrees with experimental data measured by Bouneau et al. (2002), in which the sputtering of a Au surface by Au$_n$ clusters ($n \leq 13$) with total impact energies of up to 5 MeV has been studied. In those experiments a scaling like

$$Y_n(E) = n^2 f\left(\frac{E}{n}\right), \tag{14}$$

has been found, in obvious contrast to Equation (12). The origin of this discrepancy is still under discussion. Possibly, one or several of the following issues are relevant:

1. Under the experimental conditions, the projectile may deposit its energy deeply into the material, and also in the form of subcascades, thus producing buried spikes instead of near-surface spikes in the simulations.

2. In the simulations, no electron-phonon coupling was taken into account with the reasoning that the role of electronic heat transport in the highly disordered spike region is largely unclear from a physical point of view. If, however, spike quenching by electronic heat conduction is relevant, late emission events will be strongly affected. Note, in particular, that the simulated sputter yields – in the range where simulated projectile energies and sizes coincide with the of experimental conditions – are considerably (up to one order of magnitude) larger than experimental values; this might possibly be explained by the role of spike quenching due to electronic heat conduction.
3. Interatomic interaction potentials are poorly tested in the range of high energy densities and pressures and low particle densities relevant for the spike region.

3.3. Crater Formation

Due to the high emission yields and the collective nature of the emission flow, spike sputtering is usually connected to the formation of craters. For spike sputtering in the scenario mentioned above – i.e., where the high energy deposition close to the surface leads to the phase explosion of a near-surface part of the target – crater formation is characterized by the following features (Aderjan and Urbassek, 2000; Colla et al., 2000:

1. above a threshold impact energy E_{th}, the crater volume increases linearly with the total cluster energy;
2. the crater shape is roughly hemispherical;
3. a crater rim is formed, in which the majority of the atoms excavated from the crater are deposited; the rest have been sputtered.

Aderjan and Urbassek (2000) and also Nordlund (2001) note that a similar scaling of the crater size with total impact energy is observed also for macroscopic projectile impact, such as dust particles, bullets, or meteorites.

3.4. Cluster Emission

Both experiments and molecular-dynamics computer simulations show that clusters form an important contribution to the flux of sputtered particles (Urbassek and Hofer, 1993). The abundance distribution of emitted clusters obeys a power law

$$Y(n) \propto n^{-\alpha} \tag{15}$$

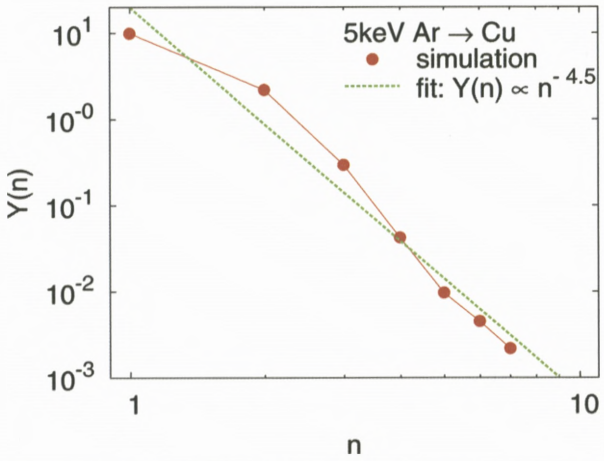

Figure 11. Abundance distribution of sputtered clusters $Y(n)$ *versus* number of atoms contained in the cluster, n. Symbols: Results from molecular-dynamics simulations of 5 keV Ar impact on a Cu (111) surface; fragmentation of metastable clusters after emission has been taken into account. Line: power-law decay, Equation (12), with $\alpha = 4.5$. Data taken from Colla et al. (1998).

in cluster size n; Figure 11 gives an example obtained by molecular-dynamics simulation. The power exponent α has been shown empirically to strongly correlate with the total sputter yield Y; it decreases with Y down to values $\alpha < 4$ and even around 2 (Samartsev et al., 2005). Note that a statistical-combination model for the formation of clusters in the flux of sputtered atoms would predict an exponential abundance distribution. Both the origin of a power-law distribution and of the reason for the strong correlation with the total sputter yield are not entirely clear. Two models exist which predict power-law distributions, albeit with fixed values of the exponent α:

1. The shock wave models mentioned above (Bitensky and Parilis, 1987) in Section 3.1 predict a value of $\alpha = 2$.
2. The gas-flow model (Urbassek, 1988) assumes cluster production to occur in thermodynamic equilibrium; then the highest abundance of large clusters is found in the vicinity of the critical point. Here clusters are distributed according to a power law (15) with α given by the critical exponents of the medium; for a van-der-Waals medium $\alpha = 7/3$.

Note that these models do not predict the power exponent to depend on the total sputter yield. Possibly, such a dependence may be due to the averaging over many impact events: The large-n tail of the distribution will be dominated by particularly

hot near-surface spikes, which abundantly produce clusters, possibly with an exponent α close to the critical value 7/3. An averaging over the properly weighted spike components may then be approximated by a power law Equation (15); the effective value of α will then be lower with increasing total average yield.

3.5. Sputtering from Swift-Ion Tracks

An interesting situation of sputtering under spike conditions occurs when particles are sputtered from a swift-ion track. Such a track is the consequence of the – more or less rectilinear – trajectory of a swift ion, which slows down in the material due to electronic stopping. The highly excited electrons along the cylindrical track impart their energy to the target atoms; for sufficiently high energy densities, a situation characterized by the spike condition, Equation (11), may be established.

Theoretical models for sputtering from these tracks have been set up, cf. the contributions by Toulemonde et al. (2006) and Klaumünzer (2006), and also molecular-dynamics simulations have been employed for investigation. These usually skip the details of how the electronic energy is converted to nuclear motion and immediately assume the excitation energy to be imparted as random kinetic energy to the atoms. The first simulations have been published by Fenyö et al. (1990), Fenyö and Johnson (1992) and Urbassek et al. (1994). More recently, Bringa and Johnson (1998) and Bringa et al. (1999a, 1999b, 2000) analyzed this scenario in greater detail. The following results could be obtained: (i) A regime was identified where at low densities of the energetic excitation events the yield is linear due to the sparse distribution of the excitations. (ii) The high-energy-density linear regime is connected to the formation of a melt and the removal of energy by a pressure pulse. In this regime the size of the yield increases with the initial radial extension of the track and is determined by the removal of energy radially by the pressure pulse and by the transport of energy to the surface.

Beuve et al. (2003) studied two further aspects of fast-ion-induced sputtering by including the dynamics of the electronic subsystem: (i) The energy transfer from the electronic to the atomic system is assumed not to occur instantaneously but to take a period of time Δt. For $\Delta t > 1$ ps it is found that the sputtering yield becomes strongly nonlinear as a function of the stopping power. (ii) The influence of a non-homogeneous spatial distribution of the electronic excitations is modelled. It is shown that such a spatial distribution also leads to a strongly non-linear dependence of the yield on the excitation density.

4. Further Topics

Among further topics in sputter theory, which are presently being investigated, I mention the following:

4.1. Electronic Excitation

Projectiles which are slowed down in the nuclear-stopping regime impart some energy to the electron system of the target; this also holds true for the energetic recoil atoms generated in the target. This energy deposition can be modelled using available quantitative schemes of electronic stopping. In fact, such simulations have been performed with the aim of predicting the probability of sputtered particles to be excited or ionized (Sroubek et al., 2003). However, it might be interesting to know about the fate of the energy given to the electronic system:

1. In metals, swift electronic heat conduction may efficiently quench the collision cascade and in particular long-lived spikes, see Section 3.2 above.
2. As the discussion on ion tracks in Section 3.5 above showed, there exist conditions where energy transfer from the electronic to the atomic system may be important.
3. Since in metals, the electronic degrees of freedom may be assumed to equilibrate quickly, the conditions of excitation and ionization of sputtered particles will be determined by the local electron temperatures around the sputtered particle positions.

Duvenbeck and Wucher (2005) are investigating the latter process by including the electron temperature as a further variable in molecular-dynamics simulations. Their results demonstrate that a detailed knowledge of the dependence of the electron heat diffusivity on the atomic environment (density, temperature, local order) is crucial for progress in this area.

4.2. Molecular Targets

A prototypical example of the sputtering of molecular targets is given by condensed diatomic gas targets (Balaji et al., 1995). Here a variety of phenomena occur beyond those existing in atomic targets:

1. The rotational and vibrational excitation of the target molecules provides a further channel for projectile energy deposition. As a consequence, the (translational) temperature in the cascade volume is smaller than in the case

of sputtering of an atomic target. This effect will reduce the sputter yield in a spike scenario.
2. The possibility of target molecule dissociation operates in the same direction.
3. Upon molecule dissociation, radicals may form and react. These reactions may be exothermic, thus releasing energy and enhancing the sputter yield.

In fact, these possibilities have been seen in experiment and interpreted in this manner by Balaji et al. (1995) and David et al. (2001). Besides the analysis presented in these papers, a detailed quantitative model has not been set up.

In the field of sputtering of organic molecules and polymers some progress has been achieved in particular by the work of Garrison, Delcorte and Postawa. They performed a series of dedicated molecular-dynamics simulations motivated by the needs of organic SIMS; for recent references cf. Czerwinski et al. (2006) for thin organic films and Delcorte et al. (2003) for polymers.

Garrison mentions in her review (2001) that the following features in the sputtering of organic, biological and polymeric solids were demonstrated in the simulations:

- formation of fragments;
- reactions between fragments (radical-radical recombinations);
- molecule emission by a collective mechanism called *molecule liftoff* (Garrison et al., 2000).

4.3. Chemical Effects

Chemical or reactive sputtering occurs when the projectile, or its reaction products, react with the target, thus forming more volatile species which enhance the sputter yield. Analogously, e.g., polymerization reactions occurring in the target and induced by the ion impact, may decrease the sputter yield. Simulations have been performed, e.g., to understand the following specific systems:

1. Schoolcraft and Garrison (1991), Feil et al. (1993) and Feil (1995) studied the reactive sputtering of silicon by halogen ions motivated by the technique of RIBE (reactive ion beaming etching)
2. The sputtering of graphite by hydrogen, motivated by interest in the use of graphite as a first-wall material of fusion reactors (Salonen et al., 2001).

5. Conclusions

In his 1980 review, Jackson poses the following questions to indicate the future directions of sputter theory:

1. What further improvements can be made in transport theory?
2. Can gas-like simulations be used in most practical sputtering calculations?
3. What information can be expected from single-knockon work?
4. Are there surface ejection spike phenomena?
5. What happens in non-linear cascades?
6. How are chunks and large clusters emitted?
7. What effect does pre-existing damage have on sputtering?

Of these, the first three have been answered such that (1) transport theory has reached a mature state of full development, (2) binary collision codes like TRIM or MARLOWE have found widespread use in predicting projectile ranges and sputtering in the collision-cascade and single-knockon regimes, and (3) the interest in near-threshold sputter processes, while of importance in several applications, such as, e.g., in plasma environments, has led to empirical sputter formulae like Equations (3)–(5). Issues 4–6 refer to spike sputtering and are still being actively investigated today. Question 7 is a major issue nowadays, since it affects the fluence dependence of surface modification and erosion, cf. Chason and Chan (2006).

Today the major open problems in sputter theory as addressed in this review can be summarized as follows:

1. *Is there a universal picture of spike sputtering?*
   The regions of validity of available models (shock wave, surface evaporation, gas flow, pressure pulse,...) need to be identified. The role of target materials parameters (in particular that of thermal properties like the critical temperature, importance of a liquid phase, but also the strength of the solid and the surface tension of the liquid) need to be explored. This task is complicated by the fluctuations inherent in the projectile slowing down process.
2. *Scaling laws for cluster impact.*
   While simulations find a scaling of the crater volume and sputter yield proportional to the total cluster energy, in agreement with experiments on macroscopic impacts, experiments with small clusters (Au_n clusters with $n \leq 13$ and total energies $E \leq 5$ MeV) find a different scaling. The origin of this discrepancy is unclear. It is also of interest to delineate more clearly

the parameter region where the energy proportionality of sputter yields and crater sizes hold.

3. *Role of target electrons.*
   While the process of energy transfer to target electrons during projectile slowing down forms a part of stopping theory, the question of how much energy is spent in electronic excitation by high-generation recoils in the collision cascade and in particular in a spike regime does not appear to be clarified. Furthermore, the question needs to be clarified of how efficiently electronic heat conduction can contribute to the quenching of spikes in metals.
4. *How realistic are long time (100 ps) molecular-dynamics simulations of late sputtering events?*
   Besides the role of electrons, also the reliability of interatomic potentials in high-temperature, high-pressure, low-density environments needs to be clarified. The role of boundary conditions to which the simulation volume is subjected may bias simulation results in particular at late times.
5. *What is the origin of the power-law abundance distributions observed for large-cluster emission in sputtering?*
   These hint at a cooperative emission process.
6. *Creation of surface topography by sputtering.*
   A quantification of the spatial dependence of adatoms and surface vacancies after single ion impact would be useful.
7. *Influence of surface topography on sputtering.*
   The ion irradiation of nano-sized objects, and even atomistic patterns like steps or adatom clusters necessitates an understanding of how surface features influence the sputtering process.
8. *Further topics: sputtering of molecular targets, chemical effects in sputtering, etc.*
   An understanding of universal mechanisms beyond the study of specific systems would be useful.

Acknowledgements

Thanks are due to Christian Anders, Yudi Rosandi, Luis Sandoval, and Steffen Zimmermann for preparing figures for this review. I am grateful to Peter Sigmund for a critical reading of the manuscript.

References

Aderjan R. and Urbassek H.M. (2000): Molecular-dynamics study of craters formed by energetic Cu cluster impact on Cu. Nucl Instrum Meth B **164–165**, 697–704

Anders C., Urbassek H.M. and Johnson R.E. (2004): Linearity and additivity in cluster-induced sputtering: A molecular-dynamics study of van der Waals bonded systems. Phys Rev B **70**, 155404-1-6

Aziz M. (2006): Nanoscale morphology control using ion beams. Mat Fys Medd Dan Vid Selsk **52**, 187–206

Balaji V., David D.E., Tian R., Michl J. and Urbassek H.M. (1995): Nuclear sputtering of condensed diatomic gases. J Phys Chem **99**, 15565–15572

Baragiola R.A. (2004): Observations of Sputtering: Survey of Observations and Derived Principles. Phil Trans Roy Soc (London) A **362**, 29

Behrisch R. (Ed.) (1981): Sputtering by Particle Bombardment I, Springer, Berlin

Behrisch R. (Ed.) (1983): Sputtering by Particle Bombardment II, Springer, Berlin

Behrisch R. and Wittmaack K. (Eds) (1991): Sputtering by Particle Bombardment III, Springer, Berlin

Beuve M., Stolterfoht N., Toulemonde M., Trautmann C. and Urbassek H.M. (2003): Influence of the spatial and temporal structure of the deposited-energy distribution in swift-ion-induced sputtering. Phys Rev B **68**, 125423

Biersack J.P. and Eckstein W. (1984): Sputtering studies with the Monte Carlo program TRIM.SP. Appl Phys A **34**, 73

Biersack J.P. and Haggmark L.G. (1980): A Monte Carlo computer program for the transport of energetic ions in amorphous targets. Nucl Instr Meth **174**, 257

Bitensky I.S. and Parilis E.S. (1987): Shock wave mechanism for cluster emission and organic molecule desorption under heavy ion bombardment. Nucl Instrum Meth B **21**, 26

Bohdansky J. (1984): A universal relation for the sputtering yield of monatomic solids at normal ion incidence. Nucl Instrum Meth B **2**, 587

Bouneau S., Brunelle A., Della-Negra S., Depauw J., Jacquet D., LeBeyec Y., Pautrat M., Fallavier M., Poizat J.C. and Andersen H.H. (2002): Very large Au and Ag sputtering yields induced by keV to MeV energy Au_n clusters ($n = 1 - 13$). Phys Rev B **65**, 144106

Bradley R.M. and Harper J.M.E. (1988): Theory of ripple topography induced by ion bombardment. J Vac Sci Technol A **6**, 2390

Bringa E.M. and Johnson R.E. (1998): Molecular dynamics study of non-equilibrium energy transport from a cylindrical track. I. Test of spike models. Nucl Instrum Meth B **143**, 513

Bringa E.M., Johnson R.E. and Dutkiewicz L. (1999a): Molecular dynamics study of non-equilibrium energy transport from a cylindrical track. II. Spike models for sputtering yield. Nucl Instrum Meth B **152**, 267

Bringa E.M., Johnson R.E. and Jakas M. (1999b): Molecular dynamics simulation of electronic sputtering. Phys Rev B **60**, 15107

Bringa E.M., Jakas M. and Johnson R.E. (2000): Spike models for sputtering: effect of the surface and the material stiffness. Nucl Instrum Meth B **164-165**, 762

Chason E. and Chan W.L. (2006): Ion-induced surface evolution in the linear instability regime: Continuum theory and kinetic Monte Carlo simulations. Mat Fys Medd Dan Vid Selsk **52**, 207–225

Colla T.J., Urbassek H.M., Wucher A., Staudt C., Heinrich R., Garrison B.J., Dandachi C. and Betz G. (1998): Experiment and simulation of cluster emission from 5 keV Ar → Cu. Nucl Instrum Meth B **143**, 284–297

Colla T.J., Aderjan R., Kissel R. and Urbassek H.M. (2000): Sputtering of Au (111) induced by 16-keV Au cluster bombardment: Spikes, craters, late emission, and fluctuations. Phys Rev B **62**, 8487–8493

Conrad U. and Urbassek H.M. (1992): Monte Carlo study of fluence dependent mixing and sputtering of isotopic targets under ion bombardment. Surf Sci **278**, 414–426

Czerwinski B., Delcorte A., Garrison B.J., Samson R., Winograd N. and Postawa Z. (2006): Sputtering of thin benzene and polystyrene overlayers by keV Ga and C60 bombardment. Appl Surf Sci **252**, 6419

David D.E., Balaji V., Michl J. and Urbassek H.M. (2001): Sputtering of condensed polyatomic gases by kilo-electron-volt-energy ions. Int J Mass Spectrom **212**, 477–489

Delcorte A., Arezki B. and Garrison B.J. (2003): Matrix and substrate effects on the sputtering of a 2 kDa molecule: Insights from molecular dynamics. Nucl Instrum Meth B **212**, 414

Donnelly S.E. (2006): Some solved and unsolved problems in transmission electron microscopy studies of radiation damage in solids. Mat Fys Medd Dan Vid Selsk **52**, 329–355

Duvenbeck A. and Wucher A. (2005): Low-energy electronic excitation in atomic collision cascades: A nonlinear transport model. Phys Rev B **72**, 115417

Eckstein W. (1991): Computer Simulation of Ion-Solid Interactions. Springer, Berlin

Eckstein W., Garcia-Rosales C., Roth J. and Laszlo J. (1993): Threshold energy for sputtering and its dependence on angle of incidence. Nucl Instrum Meth B **83**, 95

Feil H. (1995): Small free barrier and postdesorption collisions: The keys towards the understanding of reactive ion etching of silicon. Phys Rev Lett **74**, 1879

Feil H., Dieleman J. and Garrison B.J. (1993): Chemical sputtering of Si related to roughness formation of a Cl-passivated Si surface. J Appl Phys **74**, 1303

Fenyö D. and Johnson R.E. (1992): Computer experiments on molecular ejection from an amorphous solid: comparison to an analytic continuum mechanical model. Phys Rev B **46**, 5090

Fenyö D., Sundqvist B.U.R., Karlsson B.R. and Johnson R.E. (1990): Molecular-dynamics study of electronic sputtering of large organic molecules. Phys Rev B **42**, 1895

Friedrich A. (2003): Zerstäubung und Defektentstehung unter schrägem Edelgasionenbeschuss. Diploma thesis, University Kaiserslautern

Friedrich A. and Urbassek H.M. (2003): Effect of surface steps on sputtering and surface defect formation: molecular-dynamics study of 5 keV Xe^+ bombardment of Pt (111) at glancing incidence angles. Surf Sci **547**, 315–323

Gades H. and Urbassek H.M. (1992): Pair versus many-body potentials in atomic emission processes from a Cu surface. Nucl Instrum Meth B **69**, 232–241

Gades H. and Urbassek H.M. (1994a): Molecular-dynamics simulation of adatom formation under keV-ion bombardment of Pt (111). Phys Rev B **50**, 11167–11174

Gades H. and Urbassek H.M. (1994b): Surface binding energies of alloys: a many-body approach. Nucl Instrum Meth B **88**, 218–228

Gades H. and Urbassek H.M. (1995): Preferential sputtering of alloys: a molecular-dynamics study. Nucl Instrum Meth B **102**, 261–271

Garrison B.J. (2001): Molecular dynamics simulations, the theoretical partner to static SIMS experiments. In: Vickerman J.C. and Briggs D. (Eds), ToF-SIMS: Surface Analysis by Mass Spectrometry, Vol. 223, IM Publications, Chichester, UK

Garrison B.J., Delcorte A. and Krantzman K.D. (2000): Molecule liftoff from surfaces. Acc Chem Res **33**, 69

Glazov L.G. (1994a): Solution of the kinetic equation for the deposited energy distribution in the power cross section model. J Phys: Condens Matter **6**, 4181

Glazov L.G. (1994b): Solution of the kinetic equation for the deposited momentum distribution: neglecting threshold energy. J Phys: Condens Matter **6**, 10647

Glazov L.G. (1995): Solution of the kinetic equation for the deposited momentum distribution: II. Threshold energy effects. J Phys: Condens Matter **7**, 6365

Glazov L.G. (1997): Collision cascades and sputter fluxes in bounded random media. Nucl Instrum Meth B **122**, 611

Glazov L.G. and Paszit I. (2004): Applications of invariant embedding: positron backscattering from surfaces. Nucl Instrum Meth B **215**, 509

Glazov L.G., Shulga V.I. and Sigmund P. (1998): Analysis of a perfect sputter experiment. Surf Interface Anal **26**, 512

Gnaser H. and Oechsner H. (1990): Isotopic mass effects in sputtering: dependence on fluence and emission angle. Nucl Instrum Meth B **48**, 544

Grove Symposium (2004): Sputtering: past, present and future. W. R. Grove 150th Anniversary Issue. Phil Trans Roy Soc (London) A **362, no. 1814**, 1–194

Haring R.A., Pedrys R., Haring A. and de Vries A.E. (1984): Sputtering of condensed noble gases by keV heavy ions. Nucl Instrum Meth B **4**, 40

Harrison Jr. D.E. (1988): Application of molecular dynamics simulations to the study of ion-bombarded metal surfaces. Crit Rev Solid State Mater Sci **14**, S1

Hofer W.O. (1991): Angular, energy and mass distribution of sputtered particles. In: Behrisch R. and Wittmaack K. (Eds), *Sputtering by Particle Bombardment III*, 15, Springer, Berlin

Hou M. and Eckstein W. (1990): Anisotropy of momentum distributions in atomic-collision cascades generated in fcc materials. Phys Rev B **42**, 5959

Jackson D.P. (1980): The theory of sputtering. In: Varga P., Betz G. and Viehböck F.P. (Eds), Symposium on Sputtering, 2. Inst. f. Allg. Phys., Wien

Jakas M.M. (2004): Transport theories of sputtering. Phil Trans Roy Soc (London) A **362**, 139

Johnson R.E. and Evatt R. (1980): Thermal spikes and sputtering yields. Radiat Eff **52**, 187

Johnson R.E., Sundqvist B.U.R., Hedin A. and Fenyö D. (1989): Sputtering by fast ions based on a sum of impulses. Phys Rev B **40**, 49

Kelly R. (1990): Thermal sputtering as a gas-dynamic process. Nucl Instrum Meth B **46**, 441

Kitazoe Y., Hiraoka N. and Yamamura Y. (1981): Hydrodynamical analysis of non-linear sputtering yields. Surf Sci **111**, 381

Klaumünzer S. (2006): Thermal-spike models for ion track physics: A critical examination. Mat Fys Medd Dan Vid Selsk **52**, 293–328

Lo D.Y., Tombrello T.A. and Shapiro M.H. (1989): Molecular dynamics simulation of preferential sputtering from isotopic mixtures. Nucl Instrum Meth B **40/41**, 270

Michely T. and Krug J. (2004): Islands, Mounds, and Atoms, Springer Series in Surface Science, Vol. 42, Springer, Berlin

Michely T. and Teichert C. (1994): Adatom yields, sputtering yields, and damage patterns of single-ion impacts on Pt (111). Phys Rev B **50**, 11156

Möller W. and Eckstein W. (1984): TRIDYN – A TRIM simulation code including dynamic composition changes. Nucl Instrum Meth B **2**, 814

Nordlund K. (2001): Ions mimic the impact of meteorites. Phys World **14**, 22

Nordlund K., Tarus J., Keinonen J., Donnelly S.E. and Birtcher R.C. (2003): Atomic fingers, bridges and slingshots: formation of exotic surface structures during ion irradiation of heavy metals. Nucl Instrum Meth B **206**, 189

Rehn L.E., Birtcher R.C., Donnelly S.E., Baldo P.M. and Funk L. (2001): Origin of Atomic Clusters during Ion Sputtering. Phys Rev Lett **87**, 207601

Reimann C.T. (1993): Theoretical models for sputtering and desorption of large bio-organic molecules under collisional and electronic excitation by ion impact. Mat Fys Medd Dan Vid Selsk **43**, 351

Robinson M.T. and Torrens I.M. (1974): Computer simulation of atomic-displacement cascades in solids in the binary-collision approximation. Phys Rev **9**, 5008

Rosencrance S.W., Burnham J.S., Sanders D.E., He C., Garrison B.J., Winograd N., Postawa Z. and DePristo A.E. (1995): A mechanistic study of atomic desorption resulting from the keV ion bombardment of fcc (001) single crystal metals. Phys Rev B **52**, 6006

Salonen E., Nordlund K., Keinonen J. and Wu C.H. (2001): Swift chemical sputtering of amorphous hydrogenated carbon. Phys Rev B **63**, 195415

Samartsev A.V., Duvenbeck A. and Wucher A. (2005): Sputtering of indium using Au_m projectiles: Transition from linear cascade to spike regime. Phys Rev B **72**, 115417

Schoolcraft T.A. and Garrison B.J. (1991): Initial stages of etching of the silicon Si100 (2×1) surface by 3.0-eV normal incident fluorine atoms: a molecular dynamics study. J Am Chem Soc **113**, 8221

Sckerl M.W., Sigmund P. and Vicanek M. (1996): Particle fluxes in atomic collision cascades. Mat Fys Medd Dan Vid Selsk **44**, 1

Sckerl M.W., Lam N.Q. and Sigmund P. (1998): Compositional changes in alloys during ion bombardment at elevated temperatures. Nucl Instrum Meth B **140**, 75

Shapiro M.H., Tombrello T.A. and Harrison Jr. D.E. (1988): Simulation of isotopic mass effects in sputtering, II. Nucl Instrum Meth B **30**, 152

Shulga V.I. and Eckstein W. (1998): Depth of origin of sputtered atoms for elemental targets. Nucl Instrum Meth B **145**, 492

Shulga V.I. and Sigmund P. (1995): Simulation of energy-dependent isotope sputtering. Nucl Instrum Meth B **103**, 383

Shulga V.I. and Sigmund P. (1996): Analysis of the primary process in isotope sputtering. Nucl Instrum Meth B **119**, 359

Sigmund P. (1969): Theory of sputtering 1. Sputtering yield of amorphous and polycrystalline targets. Phys Rev **184**, 383

Sigmund P. (1973): A mechanism of surface micro-roughening by ion bombardment. J Mater Sci **8**, 1545

Sigmund P. (1974): Energy density and time constant of heavy-ion-induced elastic-collision spikes in solids. Appl Phys Lett **25**, 169

Sigmund P. (1981): Sputtering by ion bombardment: Theoretical concepts. In: Behrisch R. (Ed.), Sputtering by Particle Bombardment I, 9, Springer, Berlin

Sigmund P. (Ed.) (1993): Fundamental Processes in Sputtering of Atoms and Molecules (SPUT92). Mat. Fys. Medd. Dan. Vid. Selsk., **43**, Copenhagen

Sigmund P. and Claussen C. (1981): Sputtering from elastic-collision spikes in heavy-ion-bombarded metals. J Appl Phys **52**, 990

Sigmund P. and Lam N.Q. (1993): Alloy and isotope sputtering. Mat Fys Medd Dan Vid Selsk **43**, 255

Sroubek Z., Sroubek F., Wucher A. and Yarmoff J.A. (2003): Formation of excited Ag atoms in sputtering of silver. Phys Rev B **68**, 115426

Sunner J., Ikonomou M.G. and Kebarle P. (1988): SIMS spectra of alcohols and the phase explosion model of desorption ionization. Int J Mass Spectrom Ion Proc **82**, 221

Szymczak W. and Wittmaack K. (1993): Angular distributions of gold sputtered from a (111) crystal: Dependence of spot shapes and of spot and background yields on the primary ion mass and energy and on the target temperature. Nucl Instrum Meth B **82**, 220

Toulemonde M. et al. (2006): Experimental phenomena and thermal spike model description of ion tracks in amorphisable inorganic insulators. Mat Fys Medd Dan Vid Selsk **52**, 263–292

Urbassek H.M. (1988): Sputtered cluster mass distribution, thermodynamic equilibrium and critical phenomena. Nucl Instrum Meth B **31**, 541–550

Urbassek H.M. (1997): Molecular-dynamics simulation of sputtering. Nucl Instrum Meth B **122**, 427–441

Urbassek H.M. and Hofer W.O. (1993): Sputtering of molecules and clusters: Basic experiments and theory. Mat Fys Medd Dan Vid Selsk **43**, 97–125

Urbassek H.M. and Michl J. (1987): A gas-flow model for the sputtering of condensed gases. Nucl Instrum Meth B **22**, 480–490

Urbassek H.M. and Waldeer K.T. (1991): Spikes in Condensed Rare Gases Induced by keV-Atom Bombardment. Phys Rev Lett **67**, 105–108

Urbassek H.M., Kafemann H. and Johnson R.E. (1994): Atom ejection from a fast-ion track: A molecular-dynamics study. Phys Rev B **49**, 786–795

Vicanek M. (1999): Electron transport processes in REELS and XPS. Surf Sci **440**, 1

Vicanek M., Jimenez Rodriguez J.J. and Sigmund P. (1989): Depth of origin and angular spectrum of sputtered atoms. Nucl Instrum Meth B **36**, 124

Vicanek M., Conrad U. and Urbassek H.M. (1993): Energy partitioning and particle spectra in multicomponent collision cascades. Phys Rev B **47**, 617–629

Vicanek M., Sckerl M.W. and Sigmund P. (1998): Effect of composition gradients in alloys on differential sputter parameters. Nucl Instrum Meth B **140**, 61

Wahl M. and Wucher A. (1994): VUV photoionization of sputtered neutral silver clusters. Nucl Instrum Meth B **94**, 36

Wittmaack K. (1997): Energy- and angle-resolved depth of origin of isotopes sputtered from an elemental target. Phys Rev B **56**, R5701

Wittmaack K. (2003): Analytical description of the sputtering yields of silicon bombarded with normally incident ions. Phys Rev B **68**, 235211

Zimmermann S. (2006): Clusterbeschuss auf Oberflächen: Untersuchung des Fragmentations- und Zerstäubungsverhaltens. Ph.D. thesis, University Kaiserslautern

Zimmermann S. and Urbassek H.M. (2006): Sputtering of Au by cluster impact. Nucl Instrum Meth B, submitted